PITHA 08/20
SFB/CPP-08-62
TTP08-38
November 24, 2008

NLO Electroweak Corrections to Higgs Boson Production at Hadron Colliders [‡‡]

Stefano Actis [*]

Institut für Theoretische Physik E, RWTH Aachen University, 52056 Aachen, Germany

Giampiero Passarino [†]

Dipartimento di Fisica Teorica, Università di Torino, Italy INFN, Sezione di Torino, Italy

Christian Sturm [‡]

Physics Department, Brookhaven National Laboratory, Upton, NY 11973, USA

Sandro Uccirati [§]

Institut für Theoretische Teilchenphysik, Universität Karlsruhe, 76128 Karlsruhe, Germany

Results for the complete NLO electroweak corrections to Standard Model Higgs production via gluon fusion are included in the total cross section for hadronic collisions. Artificially large threshold effects are avoided working in the complex-mass scheme. The numerical impact at LHC (Tevatron) energies is explored for Higgs mass values up to 500 GeV (200 GeV). Assuming a complete factorization of the electroweak corrections, one finds a $+5\,\%$ shift with respect to the NNLO QCD cross section for a Higgs mass of 120 GeV both at the LHC and the Tevatron. Adopting two different factorization schemes for the electroweak effects, an estimate of the corresponding total theoretical uncertainty is computed.

Keywords: Feynman diagrams, Multi-loop calculations, Higgs physics

PACS classification: 11.15.Bt, 12.38.Bx, 13.85.Lg, 14.80.Bn, 14.80.Cp

---

[‡‡] Work supported by MIUR under contract 2001023713_006, by the European Community's Marie Curie Research Training Network *Tools and Precision Calculations for Physics Discoveries at Colliders* under contract MRTN-CT-2006-035505, by the U.S. Department of Energy under contract No. DE-AC02-98CH10886 and by the Deutsche Forschungsgemeinschaft through Sonderforschungsbereich/Transregio 9 *Computergestützte Theoretische Teilchenphysik*. We thank the Galileo Galilei institute for Theoretical Physics for hospitality and the INFN for partial support during the completion of this work.

[*] actis@physik.rwth-aachen.de
[†] giampiero@to.infn.it
[‡] sturm@bnl.gov
[§] uccirati@particle.uni-karlsruhe.de

1 Introduction

Gluon fusion is the main production channel for the Standard Model Higgs boson at hadron colliders. Unsurprisingly, radiative corrections have been thoroughly investigated in the past years; in particular, since next-to-leading order (NLO) QCD corrections increase the inclusive cross section for Higgs production at the LHC by a factor of about 1.5 to 1.7 with respect to the leading order (LO) term [1], there was a flurry of activity on higher order QCD effects. Recent reviews on the subject can be found in Ref. [2].

Electroweak effects are less understood than QCD ones. An early study [3] concluded that the so-called leading NLO corrections to the partonic gluon-fusion cross section $\sigma(gg \to H)$, enhanced by the squared mass of the top quark, amount to $0.4\,\%$. The size of this result is due to the delicate cancellation mechanism among various contributions described in Ref. [3], and more recent computations have shown that these corrections are not the dominant ones in the entire Higgs mass range.

Contributions induced by light quarks have been calculated in Ref. [4] and found to be extremely larger, reaching a maximum of about $9\,\%$ for a Higgs mass below 160 GeV. The terms of the amplitude involving the top quark have been evaluated in Ref. [5] by means of a Taylor expansion in the kinematic region below the WW threshold, where they partially screen the dominant effect of the light quarks. The impact of the partonic results of Refs. [4, 5] on the total cross section for Higgs production in proton-proton collisions, $\sigma(pp \to H + X)$, has been estimated for LHC energies in Ref. [6]. Assuming a complete factorization of the electroweak effects with respect to the dominant soft and collinear QCD radiation, the analysis shows that the cross section increases in a range from 4 to $8\,\%$ for a Higgs mass $M_H \leq 160$ GeV.

A satisfactory understanding of NLO electroweak effects on Higgs production at hadron colliders requires at least two additional steps: first, a detailed analysis of the WW, ZZ and $t\bar{t}$ threshold regions, looking ahead to the possible occurrence of artificially large effects associated with the opening of two-particle thresholds; second, an extension of the corrections due to the top quark to the entire Higgs mass range. Furthermore, because of the advent of the LHC, an independent derivation of the results of Refs. [4–6] for a light Higgs is certainly justified.

Improving the methods employed in Ref. [7] in the context of the Standard Model Higgs decay to two photons, we have recently completed the evaluation of all NLO electroweak corrections to the gluon-fusion Higgs production cross section at the partonic level [8], deconvoluted of the well-known QCD effects [1].

We have found that the corrections enhance the production mechanism throughout a Higgs mass range spanning from 100 GeV to about 180 GeV, where light quarks dominate and the full NLO contributions to the partonic cross section $\sigma(gg \to H)$ reach up to $6\,\%$. For higher values of M_H, instead, the corrections become negative and light quarks are not dominating; a minimum of $-4\,\%$ is reached around the $t\bar{t}$ threshold.

In addition, we have performed a dedicated study of the behavior around the WW, ZZ and $t\bar{t}$ thresholds [9], showing that unphysical singularities and large threshold effects disappear once the complex-mass scheme of Ref. [10] is applied in a two-loop context following the strategy described in Ref. [11].

In this paper we present our numerical results for the inclusive Higgs production cross section in hadronic collisions, including our own evaluation of the NLO electroweak corrections in addition to the next-to-next-to-leading order (NNLO) QCD effects [12–14]. Moreover, we provide an estimate of the residual theoretical uncertainty and perform a comparison with the impact of soft-gluon resummation at next-to-next-to-leading logarithmic (NNLL) level [15].

Our detailed numerical study is motivated by the observation that a typical size for the NLO electroweak corrections at the partonic level is 5 % for $M_{_H} = 120$ GeV; this value matches the theoretical uncertainty associated with uncalculated higher order QCD corrections, estimated to be 5 % at the LHC and 7 % at the Tevatron [16].

2 Inclusion of the NLO electroweak corrections

The inclusive cross section for the production of the Standard Model Higgs boson in hadronic collisions can be written as

$$\sigma\left(s, M_{_H}^2\right) = \sum_{i,j} \int_0^1 dx_1 \int_0^1 dx_2 \; f_{i/h_1}\left(x_1, \mu_{_F}^2\right) \, f_{j/h_2}\left(x_2, \mu_{_F}^2\right) \times$$
$$\times \int_0^1 dz \, \delta\left(z - \frac{M_{_H}^2}{s\, x_1 x_2}\right) \, z\, \sigma^{(0)} \, G_{ij}\left(z; \alpha_{_S}(\mu_{_R}^2), M_{_H}^2/\mu_{_R}^2; M_{_H}^2/\mu_{_F}^2\right), \tag{1}$$

where $\sqrt{s}$ is the center-of-mass energy and $\mu_{_F}$ and $\mu_{_R}$ stand for factorization and renormalization scales.

In Eq.(1) the partonic cross section for the sub-process $ij \to H + X$, with $i(j) = g, q_f, \bar{q}_f$, has been convoluted with the parton densities f_{a/h_b} for the colliding hadrons h_1 and h_2. The Born factor $\sigma^{(0)}$ reads

$$\sigma^{(0)} = \frac{G_{_F}}{288\sqrt{2}\pi} \left| \frac{3}{2} \sum_q \frac{1}{\tau_q} \left[1 + \left(1 - \frac{1}{\tau_q}\right) f(\tau_q) \right] \right|^2, \tag{2}$$

where $G_{_F}$ is the Fermi-coupling constant, $\tau_q = M_{_H}^2/(4M_q^2)$ and M_q is the conventional on-shell mass of the top or bottom quark; the function f is

$$f(\tau_q) = \begin{cases} \arcsin^2\sqrt{\tau_q}, & \tau_q \leq 1, \\ -\dfrac{1}{4}\left[\ln \dfrac{1 + \sqrt{1 - \tau_q^{-1}}}{1 - \sqrt{1 - \tau_q^{-1}}} - i\pi\right]^2, & \tau_q > 1 \end{cases}. \tag{3}$$

The coefficient functions G_{ij} can be computed in QCD through a perturbative expansion in the strong-coupling constant $\alpha_{_S}$,

$$G_{ij}\left(z; \alpha_{_S}(\mu_{_R}^2), M_{_H}^2/\mu_{_R}^2; M_{_H}^2/\mu_{_F}^2\right) = \alpha_{_S}^2(\mu_{_R}^2) \sum_{n=0}^{\infty} \left(\frac{\alpha_{_S}(\mu_{_R}^2)}{\pi}\right)^n G_{ij}^{(n)}\left(z; M_{_H}^2/\mu_{_R}^2; M_{_H}^2/\mu_{_F}^2\right), \tag{4}$$

with a scale-independent LO contribution given by $G_{ij}^{(0)}(z) = \delta_{ig}\,\delta_{jg}\,\delta\,(1 - z)$. The NLO QCD coefficients have been computed in Ref. [1], keeping the exact M_t and M_b dependence. NNLO results have been derived in Ref. [12] in the large M_t limit (see Ref. [17] for the NLO case); analytical expressions can be found in Ref. [13] (an independent cross-check has been reported in Ref. [14]). The accuracy of these fixed-order computations has been improved with soft-gluon resummed calculations [15, 16, 18].

The inclusion of higher order electroweak corrections in Eq.(1) requires to define a factorization scheme (relevant examples on non-factorizable effects concerning Z boson decay can be found in

Refs. [19,20]). The authors of Ref. [6] assume that the modifications induced by sub-leading higher order terms starting at three loops are small; consistently with this assumption, they completely factorize QCD and electroweak corrections at the partonic level. This ansatz is certainly well justified for $M_H \ll M_W$, where the electroweak interaction is effectively point-like.

Since our analysis spans the entire Higgs mass range, and we do not foresee the advent of a three-loop calculation involving mixed QCD and electroweak effects, we adopt a more conservative approach, and resort to the well-established LEP practice of attributing a theoretical error to the inclusion of NLO electroweak corrections [21].

We introduce two options for replacing the purely QCD-corrected partonic cross section in Eq.(1) with the expression including NLO electroweak corrections:

– CF (Complete Factorization):

$$\sigma^{(0)}\, G_{ij} \to \sigma^{(0)}\, \left(1+\delta_{\rm EW}\right)\, G_{ij}; \tag{5}$$

– PF (Partial Factorization):

$$\sigma^{(0)}\, G_{ij} \to \sigma^{(0)}\, \left[G_{ij} + \alpha_S^2(\mu_R^2)\delta_{\rm EW}\, G_{ij}^{(0)}\right], \tag{6}$$

where $\delta_{\rm EW}$ embeds all NLO electroweak corrections to the partonic cross section $\sigma(gg \to H)$,

$$\sigma_{\rm EW} = \alpha_S^2(\mu_R^2)\sigma^{(0)}(1+\delta_{\rm EW}), \tag{7}$$

with $\sigma^{(0)}$ defined in Eq.(2). The CF option of Eq.(5) amounts to an overall re-scaling of the QCD result, dressed at all orders with the NLO electroweak correction factor $\delta_{\rm EW}$; the PF option of Eq.(6) is equivalent to add electroweak corrections to QCD ones.

An intermediate option would be to fold the NLO electroweak corrections with the pure gluon-gluon NLO and NNLO QCD components; in this case $\delta_{\rm EW}$ would be convoluted with $G_{gg}^{(1)}$, but not with $G_{gq}^{(1)}$ and $G_{q\bar{q}}^{(1)}$.

Next, we define the uncertainty due to uncalculated higher order QCD corrections according to the standard method used in Ref. [15]: we vary the renormalization and factorization scales μ_R and μ_F around the natural scale of the process M_H, changing their values first simultaneously, with the bound $M_H/2 \le \mu_{R,F} \le 2\,M_H$, and then independently, with the additional constraint $\mu_R/2 \le \mu_F \le 2\,\mu_R$ at fixed μ_R. For each value of M_H, the minimal (maximal) values of the inclusive cross section of Eq.(1), associated with $\mu_{R,\rm min}$ and $\mu_{F,\rm min}$ ($\mu_{R,\rm max}$ and $\mu_{F,\rm max}$) are denoted by $\sigma^{\rm QCD}_{\rm min}$ ($\sigma^{\rm QCD}_{\rm max}$); their difference defines the QCD uncertainty band around the reference value $\sigma^{\rm QCD}_{\rm ref}$, obtained setting $\mu_R = \mu_F = M_H$.

Finally, for each set $\{M_H; \mu_{R,\rm min}; \mu_{F,\rm min}\}$, $\{M_H; \mu_R = M_H; \mu_F = M_H\}$ and $\{M_H; \mu_{R,\rm max}; \mu_{F,\rm max}\}$ we repeat the computation of Eq.(1) performing the replacements of Eq.(5) and Eq.(6). As a result, two new reference values are obtained for both CF and PF options, giving the impact of our evaluation of the NLO electroweak corrections. In addition, we obtain new minimal and maximal values for the cross section, dressed with electroweak effects, and define a new uncertainty band.

Needless to say, this procedure will only give an approximate bound on the total uncertainty; one should indeed observe that for the considered range the LO and NLO QCD bands of Ref. [1] do not overlap, with an NNLO band which is only partly contained in the NLO one.

3 Numerical results

For the NLO electroweak corrections we use our recent result [8] and consider a Higgs mass range spanning from 100 GeV to 500 GeV. In this region we cross the WW, ZZ and $t\bar{t}$ thresholds. A naive computation of the amplitude with conventional on-shell masses as input data reveals the presence of singularities at the WW and ZZ thresholds; in order to cure them, we have introduced in our computation complex masses [11], following the suggestion of Ref. [10]. The behavior at the $t\bar{t}$ thresholds, instead, is smooth, and the on-shell mass of the top quark can be safely used.

In the calculation all light-fermion masses have been set to zero and we have defined the W and Z boson complex poles by

$$s_j = \mu_j\,(\mu_j - i\,\gamma_j)\,, \quad \mu_j^2 = M_j^2 - \Gamma_j^2, \quad \gamma_j = \Gamma_j\left(1 - \frac{\Gamma_j^2}{2\,M_j^2}\right), \tag{8}$$

with $j = W, Z$. As input parameters for the numerical evaluation we have used the following values taken from Ref. [22]:

$$\begin{array}{ll} M_W = 80.398\,\mathrm{GeV}, & M_Z = 91.1876\,\mathrm{GeV}, \\ \Gamma_Z = 2.4952\,\mathrm{GeV}, & G_F = 1.16637\,\times\,10^{-5}\,\mathrm{GeV}^{-2}. \end{array} \tag{9}$$

For the mass of the top quark, we have used $M_t = 170.9\,\mathrm{GeV}$ [23]; for the width of the W boson, we have chosen the value $\Gamma_W = 2.093\,\mathrm{GeV}$, predicted by the Standard Model with electroweak and QCD corrections at one loop.

Our results for δ_{EW} defined in Eq.(7) are shown in Fig. 1, where we include the complete corrections, comprehensive of light- and top-quark contributions, in the entire range of interest. The introduction of the complex-mass scheme in our two-loop evaluation has a striking consequence, visible around two-particle thresholds, where artificial cusp effects disappear. A detailed analysis of this issue can be found in Ref. [9].

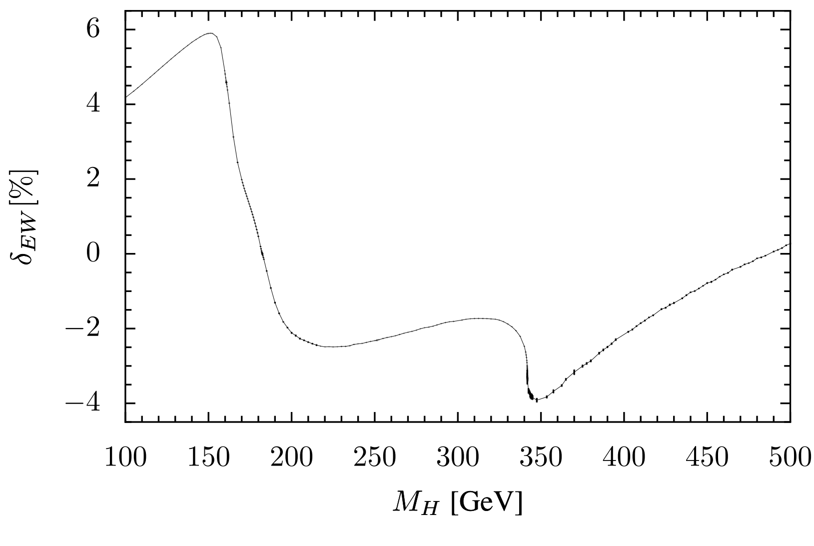

Figure 1: NLO electroweak percentage corrections to the partonic cross section $\sigma(g\,g \to H)$.

For including the NLO electroweak corrections in the hadronic cross section of Eq.(1), we have used the FORTRAN code HIGGSNNLO written by M. Grazzini (see also Ref. [24]), with QCD corrections at NNLO, interfaced with the MRST2002 set of parton distribution functions [25]. Although partially outdated, they represent the best choice for our purposes, allowing for a direct comparison with the results of Ref. [15]. In the code the parton densities, as well as the strong-coupling constant α_S, are evaluated at each corresponding order, with one-loop α_S at LO ($\alpha_S(M_Z^2) = 0.130$), two-loop α_S at NLO ($\alpha_S(M_Z^2) = 0.1197$) and three-loop α_S at NNLO ($\alpha_S(M_Z^2) = 0.1154$), as described in Ref. [15].

In the following, we will discuss our numerical results introducing K factors, defined as the ratio of the cross section including higher order corrections over the LO result. According to the discussion in Section 2, we will define K factors for NNLO QCD corrections and for NNLO QCD + NLO electroweak corrections under the assumption of complete (partial) factorization. The LO expression which normalizes each K factor will be always evaluated for $\mu_R = \mu_F = M_H$, with parton densities and α_S evolved at LO.

3.1 LHC results

We start showing our results for a LHC center-of-mass energy $\sqrt{s} = 14$ TeV. According to the standard procedure described in Section 2, an uncertainty band for the K factors is derived exploring the dependence of the cross section on the renormalization and factorization scales. In Fig. 2 we show the maximal and minimal values as a function of M_H, for 100 GeV $\leq M_H \leq$ 500 GeV, obtained including NNLO QCD corrections only (dashed lines) and NNLO QCD + NLO electroweak ones (solid lines). Note that in the second case the maximal and minimal values take into account both factorization options of Eq.(5) and Eq.(6). The pattern of the electroweak-

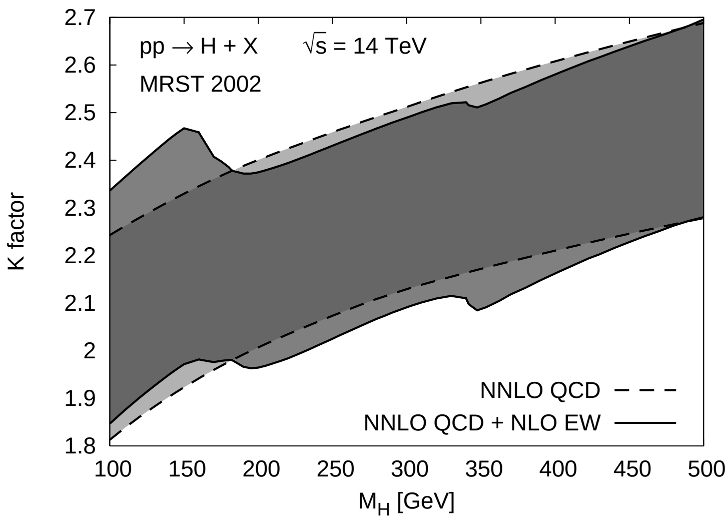

Figure 2: Uncertainty bands for the K factors for Higgs production at the LHC.

corrected uncertainty band for the K factors in Fig. 2 clearly follows the shape of the correction factor at the partonic level of Fig. 1. At about 180 GeV, when $\delta_{\rm EW}$ becomes negative, the two factorization options exchange their role: below 180 GeV, the completely (partially) factorized result fixes the upper (lower) bound, above 180 GeV the completely (partially) factorized result fixes the lower (upper) bound. This is just a consequence of the fact that the assumption of a complete factorization leads to a larger enhancement of the absolute value of the NNLO QCD corrections.

In contrast with the purely QCD-corrected K factors, we observe a higher sensitivity of the electroweak-corrected shapes of Fig. 2 on the values of the Higgs mass. The larger effect takes place at $M_H = 150$ GeV, where the QCD band at NNLO ranges from 1.92 to 2.33 and NLO electroweak effects shift it to an interval between 1.97 and 2.47.

The corresponding numerical values for the NNLO QCD-corrected cross section $\sigma^{\rm QCD}$, and the cross section including NNLO QCD + NLO electroweak corrections under the assumption of complete (partial) factorization, $\sigma^{\rm CF}$ ($\sigma^{\rm PF}$), are shown in Tab. 1, including minimal, reference and maximal values (the differences with Ref. [15] are simply due to the different values used for the top-quark mass, $M_t = 170.9$ GeV in this paper, $M_t = 176$ GeV in Ref. [15]).

Strictly speaking, the values for the QCD corrections at NNLO are given here in the large-M_t limit; however, it has been shown at NLO that this approximation is extremely good for $M_H \leq 2\,M_t$ and works with a good accuracy up to $M_H = 1$ TeV [26].

M_H	$\sigma^{\rm QCD}_{\rm min}$	$\sigma^{\rm QCD}_{\rm ref}$	$\sigma^{\rm QCD}_{\rm max}$	$\sigma^{\rm CF}_{\rm min}$	$\sigma^{\rm CF}_{\rm ref}$	$\sigma^{\rm CF}_{\rm max}$	$\sigma^{\rm PF}_{\rm min}$	$\sigma^{\rm PF}_{\rm ref}$	$\sigma^{\rm PF}_{\rm max}$
100	47.84	53.44	59.18	49.83	55.68	61.65	48.73	54.55	60.57
110	41.22	45.92	50.72	43.09	48.01	53.02	42.05	46.94	51.99
120	35.94	39.96	44.03	37.71	41.92	46.19	36.72	40.91	45.21
130	31.66	35.13	38.63	33.34	36.99	40.68	32.40	36.02	39.74
140	28.14	31.16	34.20	29.73	32.92	36.14	28.83	31.99	35.24
150	25.20	27.86	30.53	26.69	29.50	32.33	25.84	28.63	31.49
160	22.73	25.08	27.45	23.82	26.29	28.77	23.19	25.64	28.15
170	20.62	22.73	24.84	21.03	23.18	25.33	20.79	22.94	25.10
180	18.82	20.72	22.61	18.91	20.81	22.72	18.86	20.76	22.67
190	17.27	18.99	20.70	17.04	18.74	20.43	17.18	18.87	20.56
200	15.93	17.49	19.05	15.59	17.12	18.65	15.79	17.32	18.85
220	13.75	15.07	16.39	13.41	14.70	15.98	13.61	14.91	16.18
240	12.11	13.25	14.38	11.81	12.93	14.03	11.99	13.10	14.21
260	10.87	11.87	12.87	10.63	11.61	12.58	10.77	11.76	12.73
280	9.96	10.87	11.76	9.76	10.65	11.53	9.88	10.77	11.65
310	9.15	9.98	10.80	8.99	9.81	10.61	9.09	9.91	10.70
340	9.38	10.24	11.07	9.15	9.98	10.79	9.29	10.13	10.93
370	10.50	11.46	12.39	10.16	11.10	11.99	10.37	11.31	12.19
410	9.00	9.83	10.62	8.83	9.65	10.42	8.94	9.75	10.52
450	6.91	7.55	8.15	6.86	7.49	8.09	6.89	7.52	8.12
500	4.73	5.17	5.58	4.74	5.18	5.59	4.73	5.17	5.59

Table 1: NNLO QCD and NNLO QCD + NLO electroweak (with CF (Eq.(5)) and PF (Eq.(6)) options) cross sections in pb as a function of the Higgs mass in GeV at the LHC.

3.2 Tevatron results

In this section we briefly summarize the results for the Tevatron Run II, with a center-of-mass energy $\sqrt{s} = 1.96$ TeV. In Fig. 3 we show the maximal and minimal values for the K factors as a function of M_H in the range 100 GeV $\le M_H \le$ 200 GeV, obtained including NNLO QCD corrections (dashed lines) and NNLO QCD + NLO electroweak ones (solid lines). As usual, maximal and minimal values take into account both factorization options of Eq.(5) and Eq.(6). The corresponding numerical values are shown in Tab. 2.

As stressed in Ref. [15], the K factors at the Tevatron are larger than those at the LHC, because the Higgs production takes place closer to the hadronic threshold and soft-gluon effects are extremely relevant. Consequently, the impact of soft-gluon resummation is more sizeable than the electroweak effects: for $M_H = 120$ GeV, the NNLL result of Ref. [15] increases the fixed-order NNLO value by 12 %; from Tab. 2, the impact of NLO electroweak terms amounts to +5 % (+2 %) assuming a complete (partial) factorization.

Note that the same consideration is not true for the LHC, where NLO electroweak effects are comparable to those due to soft-gluon resummation at NNLL accuracy. For $M_H = 120$ GeV, we get from Ref. [15] an increase of 6 %, which matches the electroweak effects; the latter amount to +5 % (+2 %) assuming a complete (partial) factorization (see Tab. 1). Further details will be given in Section 3.4.

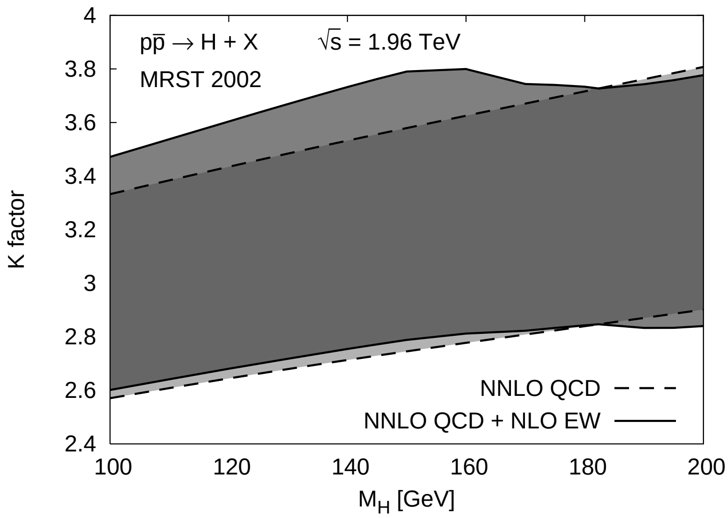

Figure 3: Uncertainty bands for the K factors for Higgs production at the Tevatron.

3.3 Threshold behavior

The scheme employed in our computation [8,9] shows that the partonic cross section $\sigma(gg \to H)$ is a smooth function of the Higgs mass; as illustrated in Fig. 1, there are no artifical large effects at the opening of two-particle thresholds.

As a consequence, unphysical cusps are avoided also at the hadronic level; in Tab. 3 we summarize the results at the LHC for values of the Higgs mass corresponding to the WW, ZZ and $t\bar{t}$ thresholds, following the same pattern of Tab. 1 and Tab. 2.

M_H	$\sigma^{\rm QCD}_{\rm min}$	$\sigma^{\rm QCD}_{\rm ref}$	$\sigma^{\rm QCD}_{\rm max}$	$\sigma^{\rm CF}_{\rm min}$	$\sigma^{\rm CF}_{\rm ref}$	$\sigma^{\rm CF}_{\rm max}$	$\sigma^{\rm PF}_{\rm min}$	$\sigma^{\rm PF}_{\rm ref}$	$\sigma^{\rm PF}_{\rm max}$
100	1.2981	1.4886	1.6829	1.3523	1.5508	1.7532	1.3136	1.5097	1.7122
110	1.0002	1.1482	1.2978	1.0455	1.2003	1.3567	1.0130	1.1656	1.3222
120	0.7833	0.9002	1.0175	0.8219	0.9445	1.0675	0.7940	0.9147	1.0380
130	0.6218	0.7153	0.8086	0.6548	0.7533	0.8515	0.6307	0.7276	0.8260
140	0.4993	0.5750	0.6500	0.5276	0.6075	0.6868	0.5068	0.5854	0.6648
150	0.4049	0.4668	0.5279	0.4288	0.4943	0.5590	0.4112	0.4755	0.5403
160	0.3314	0.3824	0.4326	0.3473	0.4008	0.4534	0.3355	0.3882	0.4408
170	0.2734	0.3158	0.3573	0.2788	0.3220	0.3644	0.2748	0.3177	0.3601
180	0.2272	0.2627	0.2974	0.2283	0.2639	0.2988	0.2275	0.2630	0.2979
190	0.1901	0.2200	0.2492	0.1876	0.2171	0.2459	0.1895	0.2191	0.2479
200	0.1601	0.1854	0.2101	0.1567	0.1815	0.2057	0.1593	0.1843	0.2084

Table 2: NNLO QCD and NNLO QCD + NLO electroweak (with CF (Eq.(5)) and PF (Eq.(6)) options) cross sections in pb as a function of the Higgs mass in GeV at the Tevatron.

M_H	$\sigma^{\rm QCD}_{\rm min}$	$\sigma^{\rm QCD}_{\rm ref}$	$\sigma^{\rm QCD}_{\rm max}$	$\sigma^{\rm CF}_{\rm min}$	$\sigma^{\rm CF}_{\rm ref}$	$\sigma^{\rm CF}_{\rm max}$	$\sigma^{\rm PF}_{\rm min}$	$\sigma^{\rm PF}_{\rm ref}$	$\sigma^{\rm PF}_{\rm max}$
160.8	22.55	24.88	27.23	23.58	26.02	28.47	22.99	25.41	27.88
182.3	18.44	20.29	22.14	18.44	20.29	22.14	18.44	20.29	22.14
341.8	9.50	10.37	11.21	9.21	10.05	10.86	9.39	10.23	11.04

Table 3: NNLO QCD and NNLO QCD + NLO electroweak (with CF (Eq.(5)) and PF (Eq.(6)) options) cross sections in pb at the two-particle thresholds at the LHC. M_H is given in GeV.

At the WW threshold, electroweak effects amount to +5% (complete factorization, CF) and +2% (partial factorization, PF) of the NNLO QCD result; around the ZZ threshold, they are vanishingly small, since here the corrections to the partonic cross section of Fig. 1 are negligible. Finally, the effect at the $t\bar{t}$ threshold is to moderately decrease the cross section, by an amount of −3% (CF) and −1% (PF).

3.4 Comparison with NNLL soft-gluon resummation

In Tab. 4 we show a comparison, for $\sqrt{s} = 14$ TeV, of our result with the NNLL resummation performed by the authors of Ref. [15]. For the NNLO QCD cross section (with and without NLO electroweak corrections) we define an average value, $\sigma_{\rm aver} = (\sigma_{\rm max}+\sigma_{\rm min})/2$, and the associated error $\Delta\sigma = (\sigma_{\rm max} - \sigma_{\rm min})/2$. Maximal and minimal values have been shown in Tab. 1; for electroweak corrections, we have taken into account both CF and PF options. The resulting electroweak shift can be directly derived from the second and third columns of Tab. 4; the NNLL shift is obtained from Tab. 1 of Ref. [15], taking the difference of the two reference values for the fixed-order and resummed computations.

M_H	$\sigma^{\rm QCD}_{\rm aver} \pm \Delta\sigma^{\rm QCD}$	$\sigma^{\rm EW}_{\rm aver} \pm \Delta\sigma^{\rm EW}$	EW shift	NNLL shift
110	45.97 ± 4.75	47.53 ± 5.49	+ 1.56	+ 2.64
130	35.15 ± 3.48	36.54 ± 4.14	+ 1.39	+ 2.04
150	27.87 ± 2.66	29.08 ± 3.25	+ 1.21	+ 1.62
170	22.73 ± 2.11	23.06 ± 2.27	+ 0.33	+ 1.34
190	18.99 ± 1.72	18.80 ± 1.76	− 0.19	+ 1.11
200	17.49 ± 1.56	17.22 ± 1.63	− 0.27	+ 1.04
220	15.07 ± 1.32	14.80 ± 1.39	− 0.27	+ 0.89
240	13.24 ± 1.14	13.01 ± 1.20	− 0.23	+ 0.79
260	11.87 ± 1.00	11.68 ± 1.05	− 0.19	+ 0.72
280	10.86 ± 0.90	10.70 ± 0.94	− 0.16	+ 0.65

Table 4: Shifts induced at the LHC on the NNLO QCD cross section by NLO electroweak effects and NNLL resummation taken from Ref. [15]. The Higgs mass is in GeV, all values for the cross section and the shifts are in pb.

We observe that for $M_H \leq 160$ GeV the inclusion of NLO electroweak corrections increases the average value of the cross section by about half the size of the QCD uncertainty half-band; the effect is comparable with the impact of soft-gluon resummation at NNLL accuracy. For higher values of the Higgs mass, NLO electroweak effects are negative, and they partially screen the impact of soft-gluon resummation on the fixed-order NNLO QCD result.

4 Conclusions

In this paper we have presented the impact of the NLO electroweak corrections to the inclusive cross section for Higgs production at the LHC.

The central value of the NNLO QCD cross section for $M_H = 120$ GeV is shifted by +5 %, both at the LHC and the Tevatron, under the assumption of a complete factorization of the NLO electroweak effects with respect to the dominant QCD radiation. The impact is relevant in view of the estimated uncertainty associated with uncalculated higher order QCD corrections, 5 % at the LHC and 7 % at the Tevatron [16]. The underlying assumption is motivated by the observation that for low Higgs masses the electroweak interaction is effectively point-like [6]. We have also derived a more conservative estimate on the electroweak shift assuming a partial factorization at leading order: for $M_H = 120$ GeV the result is reduced to +2 %.

The NNLO QCD fixed-order uncertainty bands, derived varying the renormalization and factorization scales at fixed values for the Higgs mass, have been refined including the NLO electroweak effects; as a result, they show a stronger sensitivity to the Higgs mass with respect to the pure QCD result.

For low values of the Higgs mass, we get a qualitative agreement with the results of Ref. [6], as a consequence of the light-quark dominance. For higher values of the Higgs mass, the role of the top quark becomes relevant and the agreement starts deteriorating.

We have shown that large two-particle threshold effects are avoided working in the complex-mass scheme of Ref. [10]. Further details can be found in our companion paper [9].

We have performed a detailed analysis for a wide Higgs mass range, up to 200 GeV at the Tevatron and 500 GeV at the LHC. Concerning the Tevatron, we have confirmed the expectations of Ref. [15], showing that electroweak effects are considerably smaller than those induced by the soft-gluon resummation. At the LHC, instead, the size of the positive NLO electroweak corrections is comparable to that of the positive soft-gluon resummation at NNLL; above 180 GeV, they are negative and moderately screen soft-gluon effects.

In summary, electroweak effects to Higgs production at hadron colliders are under control at NLO in the whole Higgs mass range. The main source of uncertainty is connected with a more precise knowledge of the parton distribution functions.

Acknowledgments

We gratefully thank Massimiliano Grazzini for allowing the use of the numerical program HIGGSNNLO and for useful discussions. We also acknowledge important discussions with Giuseppe Degrassi and Fabio Maltoni.

References

[1] M. Spira, A. Djouadi, D. Graudenz and P.M. Zerwas, Nucl. Phys. B **453** (1995) 17, hep-ph/9504378.

[2] S. Catani, Nucl. Phys. Proc. Suppl. **157** (2006) 202;
N.E. Adam *et al.*, report of the *Working Group on Higgs Bosons* for the workshop *Physics at TeV Colliders*, Les Houches, France, 2007, arXiv:0803.1154 [hep-ph].

[3] A. Djouadi and P. Gambino, Phys. Rev. Lett. **73** (1994) 2528, hep-ph/9406432.

[4] U. Aglietti, R. Bonciani, G. Degrassi and A. Vicini, Phys. Lett. B **595** (2004) 432, hep-ph/0404071; Phys. Lett. B **600** (2004) 57, hep-ph/0407162.

[5] G. Degrassi and F. Maltoni, Phys. Lett. B **600** (2004) 255, hep-ph/0407249.

[6] U. Aglietti, R. Bonciani, G. Degrassi and A. Vicini, contribution to the workshop *TeV4LHC*, Brookhaven, USA, 2005, hep-ph/0610033.

[7] G. Passarino, C. Sturm and S. Uccirati, Phys. Lett. B **655** (2007) 298, arXiv:0707.1401 [hep-ph].

[8] S. Actis, G. Passarino, C. Sturm and S. Uccirati, *NNLO Computational Techniques: the Cases $H \to \gamma\gamma$, gg*, in preparation.

[9] S. Actis, G. Passarino, C. Sturm and S. Uccirati, *Two-Loop Threshold Singularities, Unstable Particles and Complex Masses*, PITHA 08/21, SFB/CPP-08-63, TTP08-39.

[10] A. Denner, S. Dittmaier, M. Roth and L.H. Wieders, Nucl. Phys. B **724** (2005) 247, hep-ph/0505042;
A. Denner and S. Dittmaier, Nucl. Phys. Proc. Suppl. **160** (2006) 22, hep-ph/0605312;
A. Denner, S. Dittmaier, M. Roth and D. Wackeroth, Nucl. Phys. B **560** (1999) 33, hep-ph/9904472.

[11] S. Actis and G. Passarino, Nucl. Phys. B **777** (2007) 100, hep-ph/0612124.

[12] R.V. Harlander, Phys. Lett. B **492** (2000) 74, hep-ph/0007289;
S. Catani, D. de Florian and M. Grazzini, JHEP **0105** (2001) 025, hep-ph/0102227;
R.V. Harlander and W.B. Kilgore, Phys. Rev. D **64** (2001) 013015, hep-ph/0102241; Phys. Rev. Lett. **88** (2002) 201801, hep-ph/0201206.

[13] C. Anastasiou and K. Melnikov, Nucl. Phys. B **646** (2002) 220, hep-ph/0207004;
V. Ravindran, J. Smith and W.L. van Neerven, Nucl. Phys. B **665** (2003) 325, hep-ph/0302135.

[14] W.B. Kilgore, presented at the *31st International Conference on High-Energy Physics (ICHEP 2002)*, Amsterdam, The Netherlands, 2002, hep-ph/0208143.

[15] S. Catani, D. de Florian, M. Grazzini and P. Nason, JHEP **0307** (2003) 028, hep-ph/0306211.

[16] S.O. Moch and A. Vogt, Phys. Lett. B **631** (2005) 48, hep-ph/0508265.

[17] S. Dawson, Nucl. Phys. B **359** (1991) 283;
A. Djouadi, M. Spira and P.M. Zerwas, Phys. Lett. B **264** (1991) 440.

[18] E. Laenen and L. Magnea, Phys. Lett. B **632** (2006) 270, hep-ph/0508284;
A. Idilbi, X.d. Ji, J.P. Ma and F. Yuan, Phys. Rev. D **73** (2006) 077501, hep-ph/0509294;
A. Idilbi, X.d. Ji and F. Yuan, Nucl. Phys. B **753** (2006) 42, hep-ph/0605068.

[19] J. Fleischer, O.V. Tarasov, F. Jegerlehner and P. Raczka, Phys. Lett. B **293** (1992) 437;
G. Degrassi, Nucl. Phys. B **407** (1993) 271, hep-ph/9302288.

[20] A. Czarnecki and J.H. Kühn, Phys. Rev. Lett. **77** (1996) 3955, hep-ph/9608366.

[21] D.Y. Bardin *et al.*, report of the *Electroweak Working Group*, in CERN report 95-03, hep-ph/9709229.

[22] C. Amsler *et al.* [Particle Data Group], Phys. Lett. B **667** (2008) 1.

[23] The CDF and D0 Collaborations, FERMILAB-TM-2380-E, hep-ex/0703034.

[24] S. Catani and M. Grazzini, PoS *RADCOR2007* (2007) 046, arXiv:0802.1410 [hep-ph]; Phys. Rev. Lett. **98** (2007) 222002, arXiv:hep-ph/0703012;
M. Grazzini, JHEP **0802** (2008) 043, arXiv:0801.3232 [hep-ph].

[25] A.D. Martin, R.G. Roberts, W.J. Stirling and R.S. Thorne, Phys. Lett. B **531** (2002) 216, hep-ph/0201127; Eur. Phys. J. C **28** (2003) 455, hep-ph/0211080.

[26] M. Krämer, E. Laenen and M. Spira, Nucl. Phys. B **511** (1998) 523, hep-ph/9611272.